

Low speed/low rarefaction flow simulation in micro/nano cavity using DSMC method with small number of particles per cell

This article has been downloaded from IOPscience. Please scroll down to see the full text article.

2012 J. Phys.: Conf. Ser. 362 012007

(<http://iopscience.iop.org/1742-6596/362/1/012007>)

View [the table of contents for this issue](#), or go to the [journal homepage](#) for more

Download details:

IP Address: 95.211.165.66

The article was downloaded on 24/05/2012 at 14:00

Please note that [terms and conditions apply](#).

Low speed/low rarefaction flow simulation in micro/nano cavity using DSMC method with small number of particles per cell

Ali Amiri-Jaghargh¹, Ehsan Roohi^{1,*}, Hamid Niazmand¹ and Stefan Stefanov²

¹ Department of Mechanical Engineering, Faculty of Engineering, Ferdowsi University of Mashhad, Mashhad, Iran.

² Institute of Mechanics, Bulgarian Academy of Science, Acad. G. Bontchev Str., 1113, Sofia, Bulgaria.

Abstract. The aim of this study is to extend the validity of the simplified Bernoulli-trials (SBT)/dual grid algorithm, newly proposed by Stefanov [1], as a suitable alternative of the standard collision scheme in the direct simulation Monte Carlo (DSMC) method, for solving low speed/low Knudsen number rarefied micro/nano flows. The main advantage of the SBT algorithm is to provide accurate calculations using much smaller number of particles per cell, i.e., $\langle N \rangle \approx 1$. Compared to the original development of SBT [1], we extend the application of the SBT scheme to the near continuum rarefied flows, i.e., $Kn = 0.005$, where NTC scheme requires a relatively large sample size. Comparing the results of the SBT/dual grid scheme with NTC, it is shown that the SBT/dual grid scheme could successfully predict the thermal pattern and hydrodynamics field as well as surface parameters such as velocity slip and temperature jump. Nonlinear flux-corrected transport algorithm (FCT) is also employed as a filter to extract the smooth solution from the noisy DSMC calculation for low-speed/low-Knudsen number DSMC calculations. The results indicate that combination of SBT/dual grid and FTC filtering can decrease the total sample size needed to reach smooth solution without losing significant accuracy.

1. Introduction

Heat transfer and fluid flow in Micro/Nano-electro-mechanical systems, MEMS/NEMS, is widely gained importance due to the rapid growth of miniaturization of practical engineering and biomedical devices such as heat exchangers and chemical reactors. It is well established that the fluid behavior in MEMS/NEMS is different from their macroscopic counterpart [2]. However, due to their small dimensions, it is hard to study these behaviors experimentally. Actually, the behavior of gas gradually deviates from the thermodynamic equilibrium as the device length scale approaches the mean free path of the gas. Therefore, the numerical modeling of such devices is also problematic because the traditional Navier-Stokes (NS) equations, consistent with the near-equilibrium state, refuse to follow the realistic flow features. Knudsen number (Kn), defined as the ratio of the gas mean free path (λ) to the characteristic

* Corresponding author, Email: e.roohi@ferdowsi.um.ac.ir

length scale of the flow (L), is a good measure to characterize the departure from the equilibrium. Based on Knudsen number, the flow may appear in four different regimes [3]: continuum, slip flow, transition and free molecular regimes. For the $Kn < 0.001$, i.e., continuum regime, the NS equation with traditional no-slip boundary condition can be utilized to describe the flow behavior. In slip flow regime, $0.001 < Kn < 0.1$, the NS equation deviate from experimental results and should be accompanied with velocity slip and temperature jump boundary conditions. In the transition regime, $0.1 < Kn < 10$, flow gradually departs from the equilibrium and the NS equations are no longer valid. Finally, flow is considered as free molecular if it exceeds the limit of $Kn > 10$. Many investigations have proved the accuracy of the slip boundary conditions in slip flow regime [4]. Some researchers have tried to extend the applicability of NS equations to the early transition regime by means of developing various second order slip boundary conditions [5]. However, there is no indisputable proof to prefer one of these models among others. In addition, the concept of thermodynamic equilibrium fails to work as Kn number increases and the breakdown of the NS equations occurs [6]. Many attempts are reported to extend continuum-based equations to non-equilibrium regimes, for example, considering higher order constitutive relations for stress and heat transfer from the Chapman-Enskog expansion, moment methods are examples of such extension [7-9].

On the other hand, in contrast to continuum-based methods, molecular approach is a powerful tool to study rarefied flows. In this approach, the fluid is modeled as a collection of moving molecules interacting through collisions. DSMC method is known as one of the most successful particle-based methods in analyzing the rarefied gaseous flows. The main feature of the DSMC method, originally proposed by Bird [10], is simplifying the interaction between molecules by decoupling the motion into two successive stages of free molecular movement and binary intermolecular collision within the grid cells in each time step. It is mathematically proofed that the solution of the DSMC method converges to Boltzmann equation solution, if adequate number of particle per cells are used [11]. Bird [12] used the DSMC method to solve homogeneous gas relaxation problem. Celenligil and Moss [13] reported good agreements between the DSMC method results and experimental data of wind-tunnel for hypersonic flow over a delta wing.

Many researchers have tried to modify the DSMC method to reduce its restrictions including statistical fluctuations and computation costs. Fan and Shen [14] proposed IP method to reduce statistical fluctuations inherent in modeling of low speed microflows. Kaplan and Oran [15] used a nonlinear flux-corrected transport (FCT) filtering to exclude high frequency noise from the desired solution. Recently, some correction is suggested on the modification of the collision procedure. Stefanov [1] proposed a two-stage collision process based on the simplified Bernoulli-trials (SBT) algorithm. This method provides reasonable results with much lower number of particles per cell.

In this work, we developed a DSMC code based on Stefanov's SBT/dual grid algorithm to solve the near continuum flows, i.e., $Kn = 0.005$. Lid driven cavity flow is used as a benchmark test to check the ability of the new collision procedure in prediction of low-Knudsen low-speed flows. Additionally, we employ the nonlinear FCT filtering to reduce the statistical fluctuations of low Kn /low speed flows and reduce the computational time. Our results are compared with NTC solution and performance of the new algorithm is discussed.

2. DSMC method

DSMC is a particle method based on the kinetic theory for simulation of dilute gases. The method is carried out by modeling the gas flow using many independent simulator particles, each one representing a large number of real gas molecules in the flow field. In the DSMC method, the time step (Δt) is chosen so small that the positional changes of particles and their collisions could be decoupled for each time step. During DSMC implementation, flow field must be divided into computational cells which provide geometric boundaries and volumes required to sample macroscopic properties. Thus, the size of each cell

should be small enough that any small changes in thermodynamic properties could be captured. Cells also organize a framework to select collision pairs. The selection of collision pairs in the standard DSMC is based on the no time counter (NTC) method [16], in which the computational time is proportional to the number of simulated particles. In the NTC collision procedure, the number of particle pairs (N_c) that should be checked for a collision are

$$N_c = \frac{1}{2} f_{num} N^l < N^l > (\sigma g)_{max}^l \Delta t / \forall^l \quad (1)$$

, where f_{num} , $(\sigma g)_{max}^l$ and \forall are the ratio of number of real molecules to simulated particles, maximum of collision cross-section multiplied by particles' relative velocity and cell volume, respectively. The superscript l refers to cell l . Then, each pair (i, j) , $1 \leq i < j \leq N^l$, chosen randomly from particle subset N^l , is checked for a collision with the probability

$$p_{ij} = \frac{\sigma_{ij} g_{ij}}{(\sigma g)_{max}} \quad (2)$$

, where σ_{ij} is the effective collision cross-section of pair (i, j) and g_{ij} is the magnitude of relative velocity of pair (i, j) . The sequence of NTC collision procedure is shown in Figure 1.

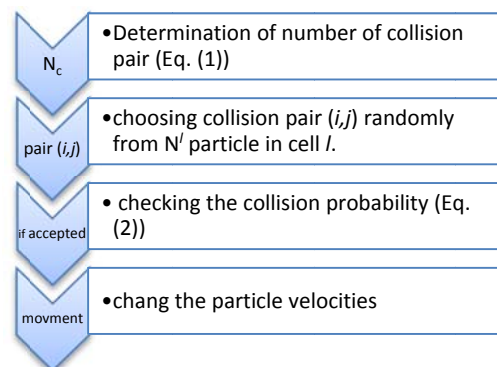


Figure 1. The NTC collision procedure

An insufficient number of particles per cell can be sources of stochastic errors which increases the number of undesirable repeated collisions in cells. However, adjusting enough particles in cells, the NTC scheme is an efficient approach for modeling the intermolecular collisions. But, it is CPU intensive in multidimensional gas flows where a huge mesh size is required for proper flow simulation. At low Knudsen numbers, in particular, using the NTC scheme necessitates the use of large number of simulated particles which greatly increases the computational cost. Recently, Stefanov [1] suggested a simplified Bernoulli trials (SBT) scheme which permits simulation with far less number of particles per cell, $< N > \sim 1$. In the SBT procedure, the particles in the l^{th} cell should be locally indexed in order to form a particle list numbered as $1 \dots N^l$. The first particle of the collision pair (i, j) , say i , is selected in sequence from the particle list, i.e., $i = 1 \dots N^l - 1$. The second particle, say j , is then selected randomly among $k = N^l - i$ particles taking place in the list after particle i .

$$j = (i + 1) + \text{int}(k \times \text{rnd}) \quad (3)$$

, where rnd refers to a random number between 0 and 1. Then each pair is checked for possible collision with the probability

$$p_{ij} = \frac{1}{2} k f_{num} \Delta t \sigma_{ij} g_{ij} / \nabla^l \quad (4)$$

It should be noted that the Δt should be adjusted so that p_{ij} rarely exceeds unity, say

$$prob\{p_{ij} \geq 1\} \rightarrow 0 \quad (5)$$

This procedure avoid the production of at least part of the eventually successively repeated collisions which occurs in Bird's NTC scheme when it is applied with a small number of particles. The theoretical background of this scheme is described in Ref. [1] by more details. The sequence of SBT collision procedure is shown in Figure 2.

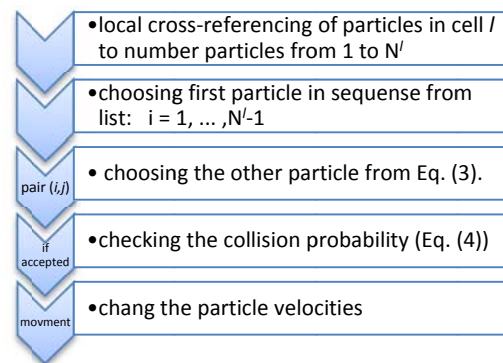


Figure 2. The simplified Bernoulli trials collision procedure

When we use small number of particles per cell, another strategy that improves the collision procedure is the usage of staggered mesh [1]. In fact, the forgoing collision procedure is applied twice in two successive half time steps, $\Delta t/2$, on a dual grid, i.e., in the first step it is applied on a standard grid, in the next step it is applied on a staggered grid which is formed by shifting all cells of the primary grid in each coordinate direction for a distance equal to half-cell size, $\Delta x/2$, $\Delta y/2$. Applying staggered grid provides the particles the chance of collision with other particles which are in a separation distance smaller than a cell size but at the first half time belongs to the adjacent cells. By translocating the cells, they become particles of one cell and will be checked for a possible collision. The steps of implementation of the staggered grid are shown in Fig. 3 where the flowchart of modified DSMC algorithm is sketched.

The results of SBT scheme are also compared with the majorant frequency scheme (MFS) [17]. MFS is an efficient collision model in the DSMC method. In this collision model, the time between two eventual collisions is evaluated from a Poisson distribution while the collisional pair is uniformly chosen from $N(N-1)/2$ available pairs in each cell. A majorant frequency which is defined as

$$v_m = \frac{N(N-1)(\sigma g)_{max}}{2 V_c} \quad (6)$$

is used to specify the Poisson distribution. More details of MFS scheme could be found in Ref. [18].

The molecular interaction is modeled by variable hard sphere (VHS) model. Monatomic argon, $m=6.63 \times 10^{-26} \text{ Kg}$ and $d=4.17 \times 10^{-10} \text{ m}$ is considered here as the gaseous medium. In order to ensure the satisfaction of the limits on the cell size, the cell dimensions Δx and Δy are considered to be 0.1λ and are

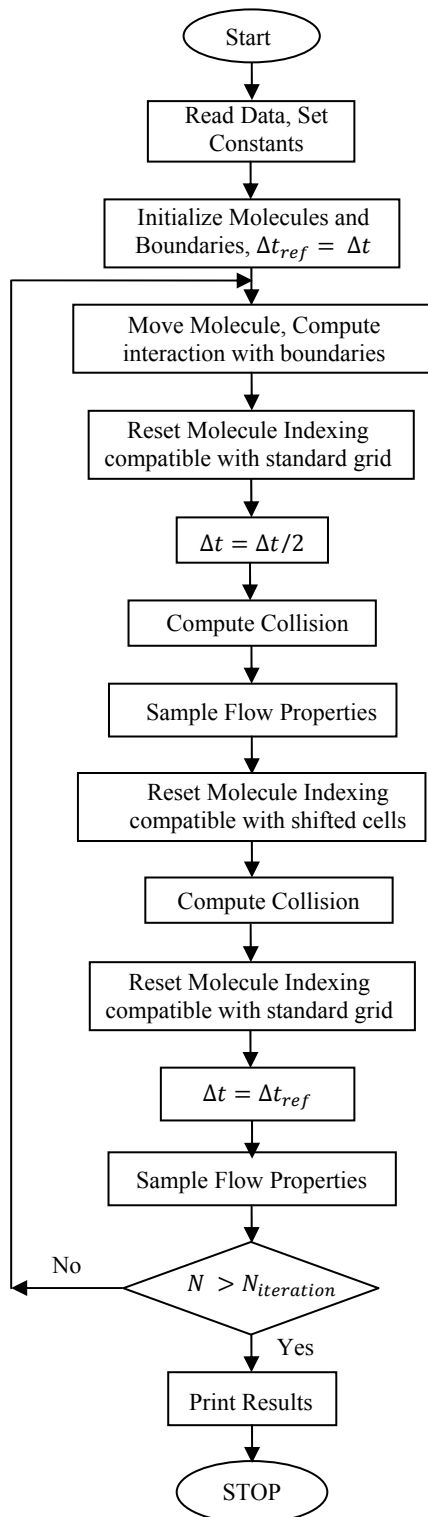


Figure 3.DSMC flowchart for staggered grid

much smaller than that for most cases. Each cell contains two molecules. All walls are treated as diffuse reflectors using the full thermal

accommodation coefficient, $\alpha = 1$. Half-range Maxwellian distribution is used to determine the velocity of reflected molecules. After achieving steady flow condition, sampling of flow properties within each cell is fulfilled during sufficient time period to avoid statistical scattering. All thermodynamic parameters such as temperature, density, and pressure are then determined from this time-averaged data. In order to minimize the scattering in the predicted results, particularly temperature, a nonlinear FCT filtering post processor is utilized [15].

3. Flux-Corrected Transport (FCT) Filtering

Modeling of low speed micro/nano flows with DSMC method encounters a serious problem of statistical fluctuations. This occurs when the bulk velocity of the flow is much smaller than the most probable thermal velocity, i.e.,

$$V_{mp} = \sqrt{2kT/m} \quad (7)$$

, where k , T and m are the Boltzmann constant, fluid temperature and molecular mass, respectively. For the present problem $V_{mp} \cong 350 \text{ m/s}$, while the lid velocity is $U_{lid} = 100 \text{ m/s}$ and the internal field velocity is much smaller below the mid line of the cavity, say of the order of 10 m/s . Therefore, the statistical noises are so great that the features of the flow may be easily lost. However, the effects of statistical noises could be reduced by increasing the sample size. In the current work, where just 2 particles in each cell are employed, the run should be continued for longer time to achieve suitable results. Additionally, following Kaplan and Oran [15], the nonlinear FCT filtering is used here as a post processing strategy to reduce statistical fluctuations and CPU run time as a result. The main feature of FCT filter, in comparison with fully diffuse simple filters, is that it makes the noisy flow converge to a solution whose correctness is already proved [15]. The FCT procedure consists of three parts: diffusion, anti-diffusion flux and anti-diffusion flux limiting. Considering the parameter ρ^0 as a noisy field that should be represented in the filtered form ρ^1 , we could write

$$\rho^0 \rightarrow \rho^d \rightarrow \rho^{dal} \equiv \rho^1 \quad (8)$$

The steps are as follows:

1) The initial values ρ^0 are diffused, giving ρ^d . This is achieved by the definition of diffusive flux of ρ at the midpoint $i + 1/2$ between ρ_i and ρ_{i+1} , $f_{i+1/2}^d(\rho)$ as

$$f_{i+1/2}^d(\rho^0) = v_{i+1/2}(\rho_{i+1}^0 - \rho_i^0) \quad (9)$$

, where $v_{i+1/2}$ are diffusion coefficients. Then

$$\rho_i^d = \rho_i^0 + f_{i+1/2}^d(\rho^0) - f_{i-1/2}^d(\rho^0) \quad (10)$$

2) To remove excess diffusion, anti-diffusion fluxes, $f_{i+1/2}^{da}(\rho)$, are defined which, however, can insert nonphysical overshoots in the solution.

$$f_{i+1/2}^{da}(\rho^d) = \mu_{i+1/2}(\rho_{i+1}^d - \rho_i^d) \quad (11)$$

, where $\mu_{i+1/2}$ are anti-diffusion coefficients.

3) To ensure stability and elimination of nonphysical overshoots, the anti-diffusion fluxes should be limited before applying to the field. This guarantees that no new maxima or minima are added to the solution. The limiter function, following Boris and Book [19] could be defined as

$$f_{i+1/2}^{dal} = S \cdot \max \left\{ 0, \min \left[S \cdot (\rho_{i+2}^d - \rho_{i+1}^d), \left| f_{i+1/2}^{da}(\rho^d) \right|, S \cdot (\rho_i^d - \rho_{i-1}^d) \right] \right\} \quad (12)$$

, where $S = \text{sgn}(\rho_{i+1}^d - \rho_i^d)$. Then

$$\rho_i^1 \equiv \rho_i^{dal} = \rho_i^d - f_{i+1/2}^{dal}(\rho^d) + f_{i-1/2}^{dal}(\rho^d) \quad (13)$$

This procedure causes the local peaks to be smoothed while keeps the value of their neighbors nearly unchanged. Actually, the effect of FCT filter can be changed by using different values of diffusion and anti-diffusion coefficients. If $\nu > \mu$ then the filter reveals a diffusive manner and depending on the degree of inequality it can smooth the peaks too fast but may do not converge to a solution. In the other side, if $\nu < \mu$ then it works as a high-frequency filter that removes the sharp peaks and converges to a solution after passing the solution from the filter for multiple times. This is shown in Figure 4 where a noisy square wave (Figure 4-a) with zero velocity is passed through the FCT filter for 1000 times (Figure 4-b) and 10000 times (Figure 4-c) for both of the forgoing cases. It is obvious that in the case of $\nu < \mu$, the filtration converges to a much less-noisier wave that never changes by more passing through the filter.

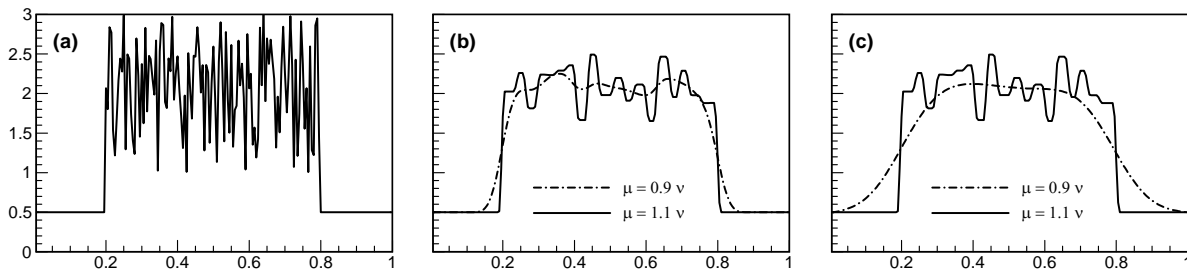


Figure 4. The effect of FCT filter on the zero velocity noisy wave,

(a) before pass

(b) 1000 passes

(c) 10000 passes

Also, in the case of $\nu > \mu$, although the filter results in smoother wave, it has a diffusive characteristic and never converges to a solution. Note that when $\nu \approx \mu$, the filter performs in a slightly diffusive manner. In this work, the diffusion and anti-diffusion coefficients are chosen as $\nu = \mu = 1/8$.

4. Grid independency test

The configuration of micro driven cavity considered in this study is shown in Figure 5 which is a square with length $L = 1 \mu\text{m}$ with a moving lid at the velocity of $U_{lid} = 100 \text{ m/s}$ and $Kn=0.005$. A grid independency study was carried out using three grids composed of 100×100 , 200×200 and 400×400 cells. Figure 6 shows the vertical component of velocity vector along the horizontal axis of the cavity, $Y/L = 0.5$.

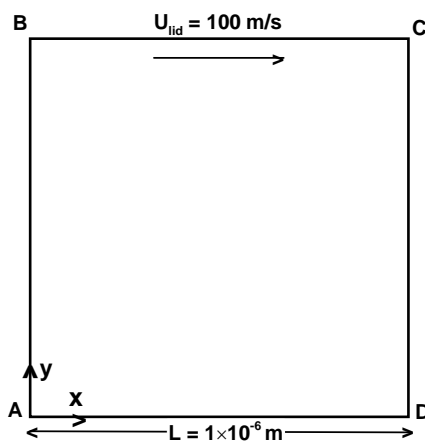


Figure 5. Geometrical configuration of micro cavity.

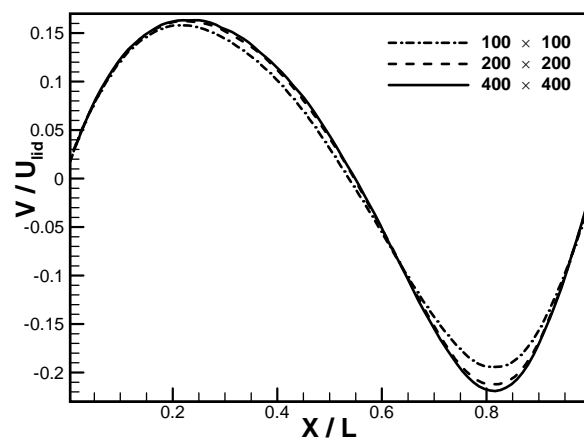


Figure 6. Grid independency test.

The results are almost equivalent for 200×200 and 400×400 grids; however the mesh size of 400×400 is selected to ensure the criterion that limits the cell size as $\Delta x \leq \frac{1}{3} \lambda$ [20].

5. Results and discussions

A micro square cavity of length $L = 1 \mu\text{m}$ with a moving lid at the velocity of $U_{lid} = 100 \text{ m/s}$ is considered. The walls temperature is set to the reference temperature, i.e., $T_w = T_0 = 300 \text{ K}$. The aim of the article is applying the DSMC method based on SBT/dual grid collision procedure in near continuum flows, i.e., $Kn = 0.005$ and compare the results with the NTC algorithm solutions. In this regard, NTC scheme is applied with various number of particles per cell to find the minimum value which leads to accurate solution. The comparison of results, which is shown in Figure 7, indicates that $\langle N \rangle = 20$ could reasonably provide the sufficient accuracy.

The ability of the SBT scheme in prediction of the cavity flow field solution is evaluated in Figures 8 and 9 where SBT results for $\langle N \rangle = 2$ are compared with those of NTC with $\langle N \rangle = 20$. In Figure 8, the dimensionless y-component of the velocity vector, V/U_{slip} , is plotted along the horizontal axis of the cavity ($Y/L = 0.5$). Also, the dimensionless x-component of the velocity vector, U/U_{slip} , is plotted along the vertical axis of the cavity at $X/L = 0.5$. The figure shows reasonably good agreement between the SBT and NTC results in prediction of the velocity field. A better assessment of the SBT scheme could be achieved if we plot the temperature field which is a square function of molecular velocity and is more sensitive to the statistical fluctuations. The temperature profile along the vertical cavity axis at $X/L = 0.5$

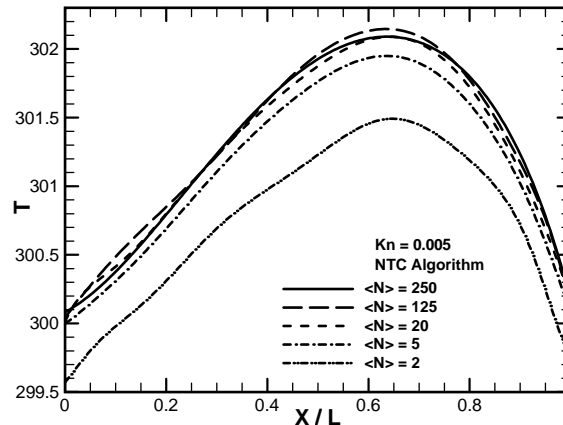


Figure 7. Effect of number of particle per cell in the accuracy of the NTC collision scheme.

is shown in Figure 9. The figure indicates that the SBT scheme with 2 particles per cell could reasonably follow the results of the NTC scheme as well as MFS with more particles. The results of NTC scheme with two particles in each cell is also plotted in this figure to emphasize on the inadequacy of this scheme at low number of particles per cell, which may locally happen in a flow with notable density gradients. In addition, although the MFS also works efficiently with small number of simulators, this figure shows that it does not guaranty the reasonable accuracy in comparison with the SBT scheme. In fact, repeated collisions may occur in the MFS scheme. This could be the source of slight deviations between the results of MFS and SBT for small number of simulators.

It should be noted that although the lid velocity is 100 m/s which correspond to a Mach number of $Ma \approx 0.3$ the flow can be strongly considered as low velocity field. The contours of local Mach number calculated with SBT scheme is shown in Figure 10. The figure indicates that the most parts of the flow field correspond to a Mach number of $Ma \leq 0.1$.

The relative computation times for the runs performed by the NTC and SBT algorithms are shown in Table 1. For the purpose of generality, the reported times are normalized by the required solution time for

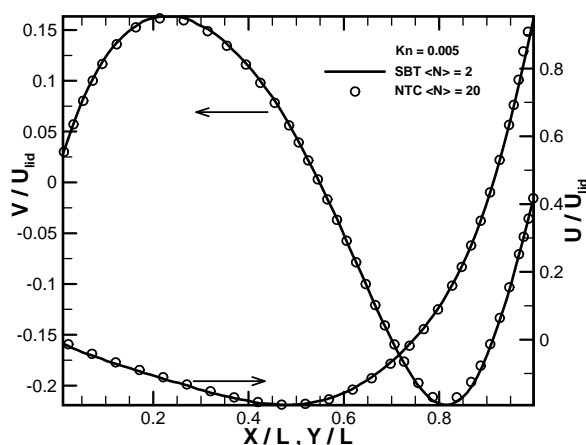


Figure 8. Comparison of the SBT and NTC schemes in prediction of flow field.

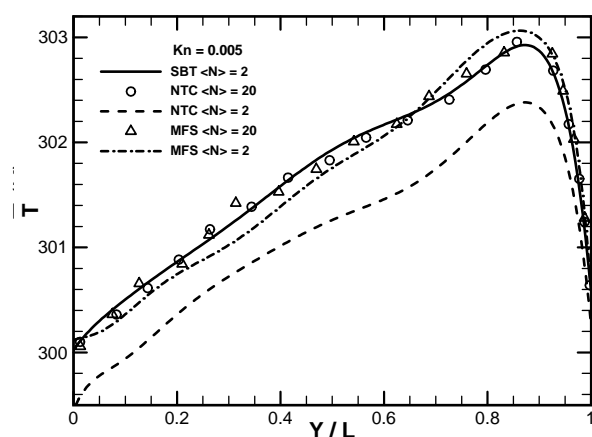


Figure 9. Comparison of the SBT with NTC and MFS schemes in prediction of thermal pattern.

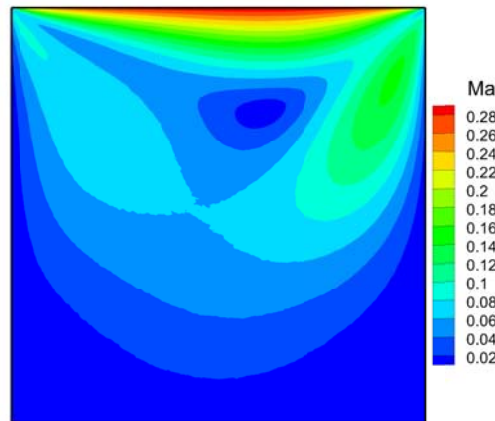


Figure 10. Contours of local Mach number calculated with SBT scheme.

NTC algorithm with $\langle N \rangle = 20$. The computational time are calculated for equal sample size, i.e., $N_{tot}N_s = cons.$, where N_{tot} and N_s are the total number of particles in the domain and the number of sampling, respectively.

Table 1. Relative computational time

	$\langle N \rangle$	time
Algorithm SBT	2	0.91
Algorithm NTC	250	1.15
	125	1.07
	20	1
	5	0.98
	2	0.75

The data of Table 1 indicate that the SBT algorithm needs less CPU time compared to the NTC to accumulate the same sample size. In addition, whereas the N_{tot} in SBT algorithm is much smaller than the NTC algorithm, say $N_{tot,SBT} = 0.4N_{tot,NTC}$ for case $\langle N \rangle = 20$; equality of the sample size in the comparison means that the number of sampling in SBT method is remarkably higher. Our numerical experiences reveal that in case of equal sample size, the more time iterating the less statistical fluctuations remain in the solution. This is consistent with the improvement of the DSMC solution in each time step that means more correct data will be accumulated as iteration advances. For example, for the cases mentioned in Table 1, the NTC algorithm for case $\langle N \rangle = 20$ was iterated for about 3,400,000 times in a mesh of 200×200 with two subcells in each direction while the SBT algorithm was iterated for about 8,500,000 times in a mesh of 400×400 without any sub-cell (actually SBT scheme needs no sub-cell) to forms the same sample size. However, the SBT does not only take less CPU time, but also results in more smooth solution.

Another feature which should be noted in further developments of the SBT scheme is the percentage of the CPU time that is consumed by different steps of the DCMC algorithm. This is mentioned in Table 2 where the NTC data are presented for comparison purpose. The relative time consumption of each DSMC step with respect to the collision is also reported to introduce a better comparison between each step as

well as between SBT and NTC schemes. The most time consuming step in the SBT scheme is indexing, which is due to using the staggered mesh that necessitates the indexing step to be applied three times at each time step, see Figure 3. Therefore, any refinement of indexing process can notably improve the speed of SBT scheme.

Table2. Percentage of CPU time usage in DSMC steps.

	SBT		NTC $\langle N \rangle = 20$	
	%	relative	%	relative
Movement	15	0.58	21	0.57
Indexing	32	1.23	18	0.49
Collision	26	1	37	1
Sampling	22	0.85	23	0.62
Other	5	0.19	1	0.03

The contours of x-component of the velocity vector is shown in Figure 11 for both the SBT (Figure 11-a) and NTC (Figure 11-b) approaches. This figure indicates that the results are in good agreement with each other. In addition, the streamlines are plotted in Figure 11. The flow consists of a large primary vortex which is followed by two small secondary vortex at corners A and D. Even though we used small number of particles per cell in SBT, we had detected the secondary vortices as well. Secondary vortices disappear at higher Kn numbers. The position of the main vortex is interested by researchers and usually is used as a validity parameter. Both of the SBT and NTC algorithms predict the primary vortex center at (0.61, 0.75).

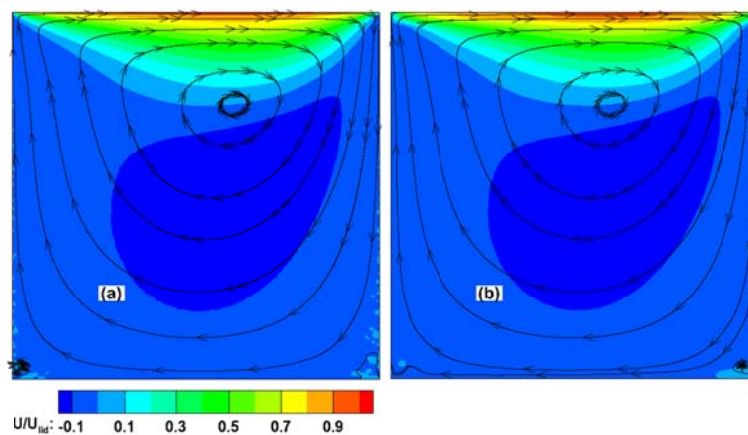


Figure 11. Comparison of x-velocity and stream lines for
(a) SBT scheme (b) NTC scheme $\langle N \rangle = 20$

Until here, it is proofed that the SBT scheme could predict the thermal and hydrodynamic patterns as accurate as the NTC scheme. But, as a result of improvement of stochastic modeling, the SBT scheme is allowed to use significantly less particle per cell at low Kn/low velocity flows. Another feature of rarefied flows which is usually interested by the researcher is the surface parameters such as velocity slip and

temperature jump. In DSMC method, the slip/jump phenomena could be evaluated based on the sampling of the corresponding molecular properties of all the particles that strike the wall surface. Following Ref. [21], the formulations for velocity slip and temperature jump are:

$$u_{slip} = \frac{\sum \left(\frac{m}{|v_p|} u_p \right)}{\sum \left(\frac{m}{|v_p|} \right)} \quad (14)$$

$$T_{gas} - T_{wall} = \frac{1}{3R} \frac{\sum \left(\frac{1}{|v_p|} \|U_p\|^2 \right) - \sum \left(\frac{1}{|v_p|} \right) u_{slip}^2}{\sum \left(\frac{1}{|v_p|} \right)} \quad (15)$$

, where p stands for particle and the summation is taken over all particles striking the wall of the regarding cell. $|v_p|$, $\|U_p\|$ and R are the absolute values of the normal velocity, velocity magnitude, i.e.,

$\|U_p\| = \sqrt{u_p^2 + v_p^2 + w_p^2}$, and gas constant, respectively. Therefore, the slip velocity is accumulated based

on the change in particle velocity due to the collision to the surface considering that the particles collide to wall with probability of $1/v_p$. From Equation (14), the temperature jump is proportional to a fraction of total kinetic energy. The velocity slip and temperature jump along the driven lid, computed by SBT and NTC schemes are plotted in Figure 12.

As observed in Figure 11, good conformity of results of SBT scheme with those of NTC indicates that the SBT model is powerful in prediction of the surface parameters as well as inter-domain features.

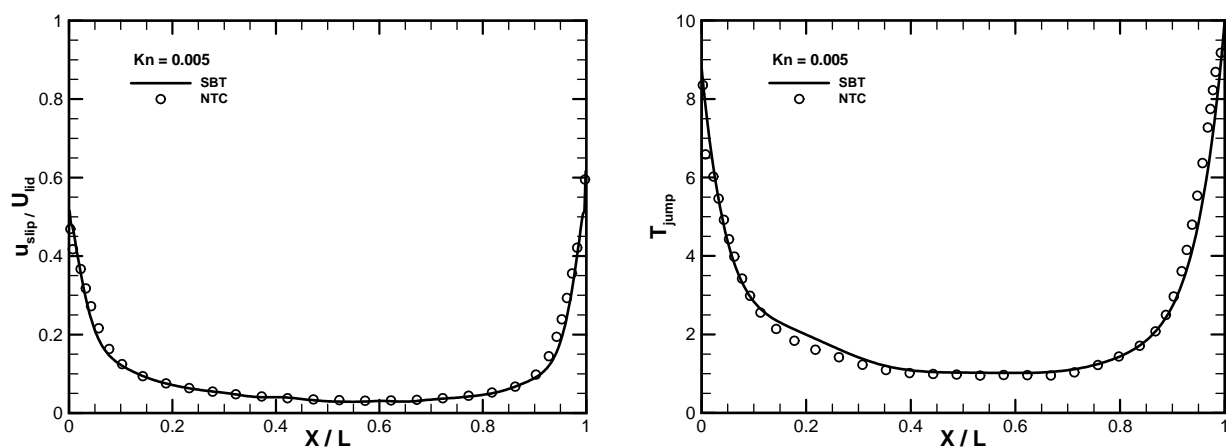


Figure 12. Velocity slip (left) and Temperature jump (right) along the driven lid computed by SBT and NTC schemes.

The performance of FCT filter is evaluated in Figure 13. This figure consists of three contour layers: the flood contour shows an unfiltered intermediate solution, after filtration this solution is shown with bold blackline contours, and the red line contour represent the filtered final solution. The filtered solution is passed through the filter for 5000 times for both cases. From the figure, it is easily realized that the FCT

filter has a key role on the removal of statistical scatters from the DSMC solution. The comparison of red and black line contours offers that the solution could be interrupted at early times without dropping much accuracy. Note that it takes us about 240 hours to reach the final solution from the intermediate solution. In the other words, this huge computational cost could be removed if we suitably employ the FTC filtering.

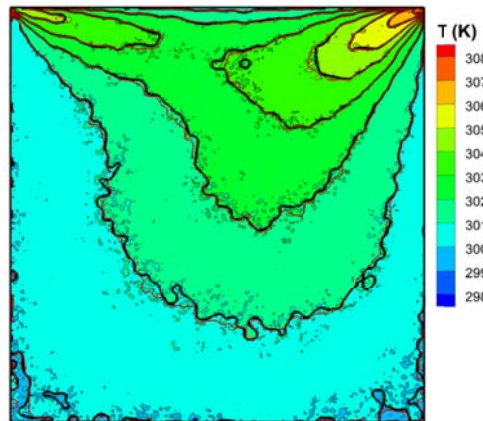


Figure 13.Ability of FCT filtering in removing stochastic noises

Flood contours: unfiltered early solution, Black line: filtered early solution, Red line: final filtered solution

6. Conclusions

DSMC Simulation of low-speed/low-Knudsen rarefied flows at micro/nano scales remains a challenge for researchers due to large computational requirements and noisy final solutions. Even though there are some suggestions to replace the basic DSMC algorithm with alternative schemes, i.e., IP scheme, these alternative schemes are not fully validated for a wide classes of problems and their derivations are case-dependent. In this work, we suggested a combination of simplified Bernoulli trial (SBT) algorithm and dual grid strategy, recently proposed by Stefanov, and nonlinear flux-corrected transport algorithm (FTC) filtering, to simulate low-speed/low-Knudsen rarefied flows at micro/nano scales efficiently. The main advantage of the proposed strategy is that it allows accurate calculations using much smaller number of particles per cell, i.e., $\langle N \rangle \approx 2$, and less computation time compared to the standard NTC scheme. We tested cavity flow at $Kn=0.005$ and showed that our SBT solution for velocity and temperature fields agrees well with standard solution with $\langle N \rangle \approx 20$, while the computational time of the SBT is around 0.91 of the NTC. Additionally, the use of FTC filtering provided correct smooth solution with less computational time compared to the basic SBT algorithm.

REFERENCES

- [1] Stefanov, S.K., 2011. "On DSMC calculation of rarefied gas flows with small number of particles in cells". *SIAM J. Sci. comput.*, Vol. 33 (2), pp. 677-702.
- [2] Beskok, A. and Karniadakis, G.E., 1999. "A model for flows in channels, pipes and ducts at micro and nano scale". *J. Microscale Thermophys. Eng.*, Vol. 3, pp. 43-77.
- [3] Schaaf, S.A. and Chambre, P.L., 1961. "Flow of Rarefied Gases". Princeton University press, USA.
- [4] Karniadakis, G., Beskok, A., and Aluru, N., 2005. "Microflows and Nanoflows: fundamentals and simulation". Springer-Verlag, New York.

- [5] Barber, R.W. and Emerson, D.R., 2006."Challenges in modeling gas-phase flow in microchannels: from slip to transition". *Heat Transfer Engineering*, Vol. 27 (4), pp.3-12.
- [6] Mizzi, S., Emerson, D.R., and Stefanov, S.K., 2007."Effect of rarefaction on cavity flow in the slip regime". *Journal of computational and theoretical nanoscience*, Vol. 4 (4), pp. 817-822.
- [7] Chapman, S. and Cowling, T.G., 1991. "The mathematical theory of non-uniform gases: an account of the kinetic theory of viscosity, thermal conduction and diffusion in gases". 3rd ed., Cambridge university press, Cambridge, UK.
- [8] Grad, H., 1949."On the kinetic theory of rarefied gases". *Communication on pure applied mathematics*, Vol. 2 (4), pp. 331-407.
- [9] Kogan, M.N., 1969."Rarefied gas dynamics". 1st ed., Plenum press, New York.
- [10] Bird, G.A., 1976."Molecular Gas Dynamics". Clarendon Press, Oxford.
- [11] Wagner, W., 1992. "A convergence proof for Bird's direct simulation Monte Carlo method for the Boltzmann equation". *J. Statist. Phys.*, Vol. 66, pp. 1011–1044.
- [12] Bird, G.A., 1963."Approach to translational equilibrium in a rigid sphere gas". *Physics of fluids*, Vol. 6 (10), pp. 1518.
- [13] Celenligil, M.C. and Moss, J.N., 1992."Hypersonic rarefied flow about a delta wing direct simulation and comparison with experiment". *AIAA journal*, Vol. 30 (8), pp. 2017-2023.
- [14] Fan, J. and Shen, C., 2002."Micro-scale gas flows". *Adv. Mech.*, Vol. 32, pp. 321-336.
- [15] Kaplan, C.R. and Oran, E.S., 2002."Nonlinear filtering for low-velocity gaseous microflows". *AIAA Journal*, Vol. 40, pp. 82-90.
- [16] Bird, G.A., 1994."Molecular gas dynamics and the direct simulation of gas flows", 2nd ed., Oxford university press, Oxford.
- [17] Ivanov, M.S. and Rogasinsky, S.V., 1988. "Analysis of the numerical techniques of the direct simulation Monte Carlo method in the rarefied gas dynamics". *Soviet J. Numer. Anal. Math. Modelling*, Vol. 3(6), pp. 453-465.
- [18] Ivanov, M.S., Markelov, G.N. and Gimelshein, S.F., 1998. "Statistical Simulation of Reactive Rarefied Flows: Numerical Approach and Applications". AIAA Paper 98-2669.
- [19] Boris, J.P and Book, D.L, 1997."Flux-corrected transport: I. SHASTA, a fluid transport algorithm that works". *Journal of computational physics*, Vol. 135, pp. 172–186.
- [20] Alexander, F.J., Garcia, A.L. and Alder, B.J., 1998. "Cell size dependence of transport coefficients in stochastic particle algorithms". *Physics of Fluids*, Vol. 10 (6), pp. 1540-1542.
- [21] Lofthouse, A.J., 2008, PhD Thesis, University of Michigan.